

Supporting information

Iodide Mediated Reductive Decomposition of Diazonium Salts: Towards Mild and Efficient Covalent Functionalization of Surface- Supported Graphene

Yuanzhi Xia,^a Cristina Martin,^{b,c} Johannes Seibel,^a Samuel Eyley,^c Wim Thielemans,^c Mark van der Auweraer,^a

Kunal Mali^{a} and Steven De Feyter^{a*}*

^aDepartment of Chemistry, Division of Molecular Imaging and Photonics, KU Leuven, Celestijnenlaan 200F, B-3001 Leuven, Belgium, ^bDepartamento de Química Física, Facultad de Farmacia, Universidad de Castilla-La Mancha, 02071 Albacete, Spain, ^cDepartment of Chemical Engineering, Sustainable Materials Lab, KU Leuven, campus Kulak Kortrijk, Etienne Sabbelaan 53, 8500 Kortrijk, Belgium

Corresponding author: kunal.mali@kuleuven.be, steven.defeyter@kuleuven.be

Contents:

1. Experimental methods.
2. A schematic showing the functionalization process (Figure S1).
3. Comparison of the efficiency of covalent grafting achieved in this work with some literature reports together with comparison of the experimental conditions (Table S1).
4. Raman spectra of functionalized SLG on different substrates (Figure S2).
5. XPS survey spectra of pristine and functionalized SLG/SiO₂ (Figure S3).
6. Data derived from carbon 1s high resolution XPS spectrum of the SLG/SiO₂ samples (Table S2).
7. High resolution nitrogen 1s XPS spectrum of NBD functionalized SLG/SiO₂ (Figure S4).
8. Data for nitrogen 1s XPS spectrum of NBD functionalized SLG/SiO₂ (Table S3).
9. AFM images showing the edge of functionalized SLG-Si and the corresponding topographical line-profiles reflecting the layer thickness of functionalization layer (Figure S5).
10. Additional AFM and STM data for the dependence of reaction time on covalent grafting (Figure S6).
11. Raman spectrum of the pristine HOPG surface prior to functionalization (Figure S7).
12. Representative AFM data showing how the average layer thickness was obtained (Figure S8).
13. Comparison of layer thickness measured across unfunctionalized and scratched areas (Figure S9).
14. AFM data for the films obtained using long reaction times (30 min) (Figure S10).
15. STM and Raman data for the spontaneous reaction of NBD with the HOPG surface (Figure S11).
16. Additional AFM data for the concentration dependence of covalent grafting (Figure S12).

17. Variation in the surface coverage of the covalently grafted film as a function of NBD concentration obtained from AFM data (Figure S13).
 18. Additional AFM data for the [KI]/[NBD] solution mole ratio on covalent grafting (Figure S14).
 19. Characterization of the reaction mixture (NBD + KI) using UV-Vis spectroscopy (Figure S15).
 20. The time evolution of the UV-vis absorbance of the reaction mixture at different [KI]/[NBD] ratios in aqueous solution (Figure S16).
 21. Time-dependent evolution of the absorbance of NBD in aqueous solution (Figure S17).
 22. UV-Vis absorption spectrum of aqueous NBD as a function of time (monitored over a period of 1.5 hours) (Figure S18).
-

Experimental section:

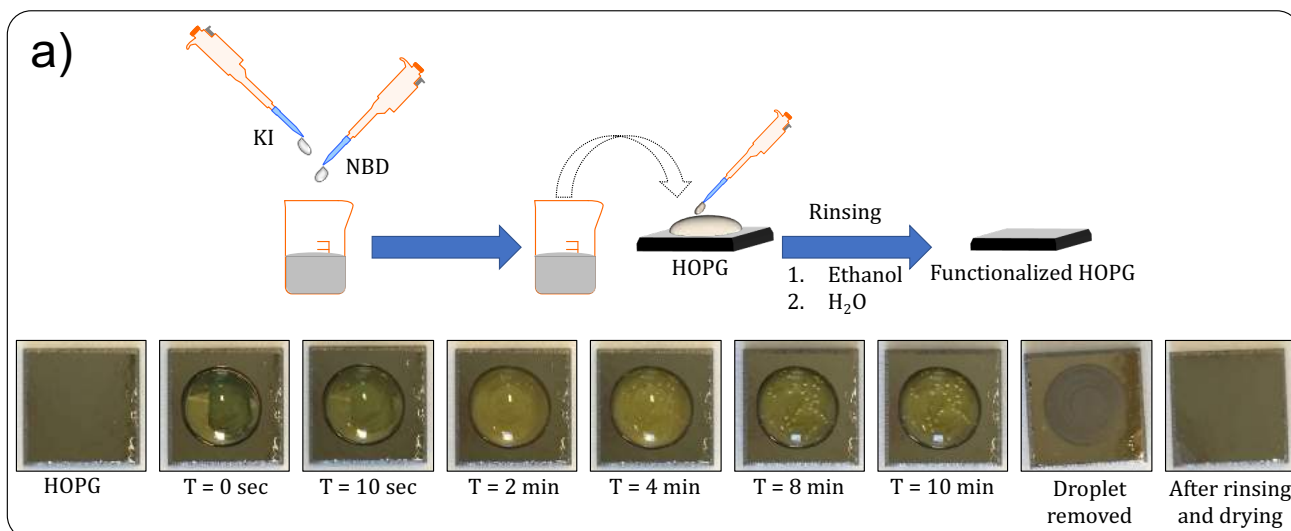
Materials. 4-Nitrobenzenediazonium (NBD) tetrafluoroborate (97%) and potassium iodide (KI) (99.9 %) were purchased from Sigma-Aldrich. All chemicals were used without further purification. High purity water (Milli-Q, Millipore, 18.2 M Ω ·cm) was used for all the experiments. The highly ordered pyrolytic graphite (HOPG, grade ZYB, Advanced Ceramics Inc., Cleveland, USA) substrates were freshly cleaved before use. CVD-grown graphene samples (1 × 1 cm²) transferred to Si ++/SiO₂ (300 nm), SLG/Au and SLG/Cu were obtained from Graphenea and were used as received.

Covalent functionalization experiments. Appropriate amounts of the diazonium salt and KI were dissolved in Milli-Q water to prepare the solutions with the desired molar concentration. The reaction mixture was prepared prior to use by mixing 100 μ L diazonium salt solution with 100 μ L KI solution in a glass vial. Immediately after mixing, 100 μ L of the mixed solution was drop casted onto freshly cleaved HOPG/graphene surface. After a given time, the reaction was stopped by rinsing with the HOPG surface with ethanol followed by water and the rinsing was repeated three times. The HOPG/graphene substrates were dried under a stream of argon.

AFM and STM characterization. AFM imaging was performed with a Cypher ES (Asylum Research) system at 32 °C in tapping mode at the air/solid interface. OMCL-AC160TS-R3 probes (spring constant ~26 N/m) with a resonance frequency around 100 kHz were used. All STM experiments were performed at room temperature (21–23°C) using a PicoLE (Keysight) machine operating in constant-current mode STM tips were prepared by mechanical cutting of Pt/Ir wire (80%/20%, diameter 0.25 mm). Scanning Probe Imaging Processor (SPIP 6.3.5) software from Image Metrology ApS was used for AFM and STM image processing. The experiments were repeated in 2–3 sessions using different tips to check for reproducibility and to avoid experimental artefacts, if any.

Raman spectroscopy. Raman experiments were performed at room temperature (21–23 °C) using an OmegaScope™ 1000 (AIST-NT). Laser light from a He–Ne laser (632.8 nm) was reflected by a dichroic mirror (Chroma, Z633RDC) and then focused onto the sample surface by using an objective (MITUTOYO, BD Plan Apo 100×, N.A. 0.7). The optical density at the sample surface was about 800 kW cm⁻². Raman scattering was collected with the same objective and directed to a Raman spectrograph (Horiba JY, iHR-320) equipped with a cooled charge-coupled device (CCD) camera operating at –100 °C (Andor, DU920P) through the dichroic mirror, a pinhole and a long pass filter (Chroma, HQ645LP). Accumulation time for all spectra was 6 s. For functionalized HOPG/graphene samples, point spectra were obtained on at least 9 different locations that are separated from each other by at least a millimeter.

UV/Vis spectroscopy. The UV-Vis absorption spectra were recorded using a Lambda 950 spectrophotometer with blocked beam and blank corrections. For monitoring the reaction between NBD and KI, 300 µL each of NBD and KI solutions were mixed together at appropriate mole ratios and the mixed solution was quickly transferred to a thin quartz cell (0.1 cm × 1 cm × 4 cm). The cell was placed into the UV-vis spectrometer to monitor the reaction by continually taking an absorption spectrum every 3 minutes.



Functionalized SLG/SiO₂

Pristine SLG/SiO₂

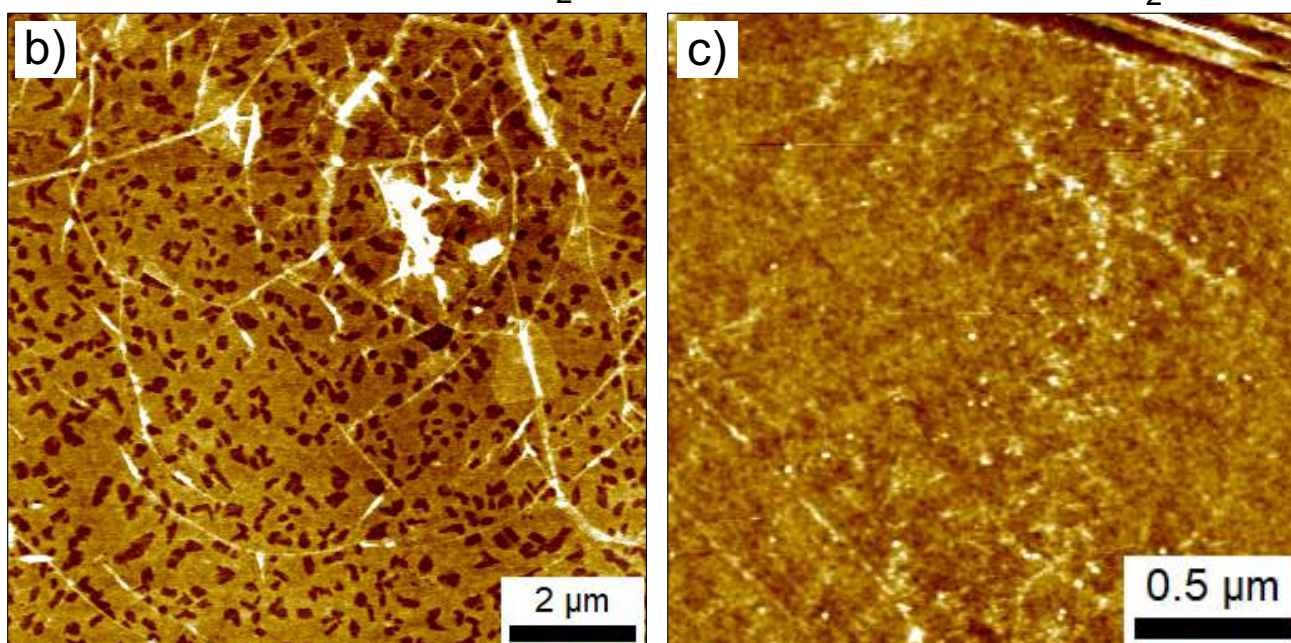


Fig. S1. A schematic showing the covalent functionalization protocol in the case of HOPG. Prior to drop casting on to the HOPG surface, the aqueous NBD and KI solutions with appropriate concentrations were mixed in a glass vial. The mixed solution was immediately drop casted on to a freshly cleaved HOPG surface. After a given time, the reaction was stopped by rinsing the surface with ethanol followed by water and the rinsing was repeated three times. The HOPG/graphene substrates were dried using argon and then subjected to further characterization. Pictures in the lower part of the figure show the evolution of nitrogen gas bubbles immediately after drop casting of the reaction mixture. Reaction conditions: 10 mM NBD + 10 mM KI, reaction time = 10 minutes. (b, c) Representative AFM images for the NBD functionalized and pristine SLG/SiO₂ surfaces, respectively.

Table S1. Comparison of the I_D/I_G values obtained for functionalized SLG/SiO₂ in this work with those reported in the literature together with reaction conditions used. See references at the bottom of the document.

	I_D/I_G	Reaction time	Temperature	Solvent	Environment
This work	3	10 min	RT	Water	Ambient conditions
Ref. 1	2,8	1 h 30 min and 15 min	RT	Ethanol	Glovebox (<0.1 ppm O ₂ , <0.1 ppm H ₂ O, Ar)
Ref. 2	1,4	16h 30 min	30 °C	Water	Ambient conditions
Ref. 3	1,2	3 Days	RT	1,2-DME	Ar purging/Strict exclusion of air or moisture
Ref. 4	1,2	20 h	150 °C	THF	Glovebox (<0.1 ppm O ₂ , <0.1 ppm H ₂ O, Ar)
Ref. 5	0,8	20 h	RT	CH ₃ CN	N ₂ -purged
Ref. 6	1,1	48 h	RT	DME	Glovebox (<0.1 ppm O ₂ , <0.1 ppm H ₂ O, Ar)

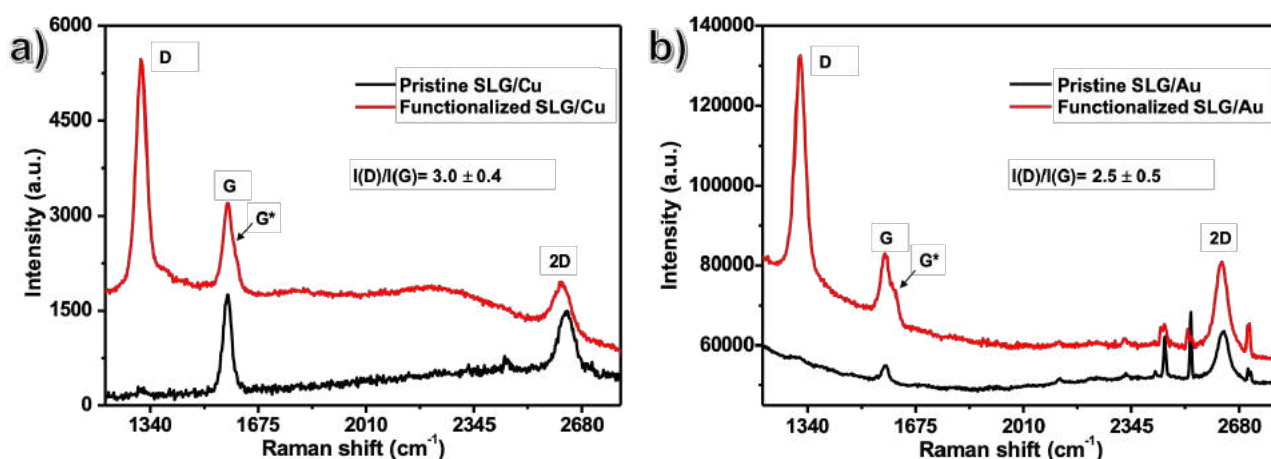


Fig. S2. Raman spectra of functionalized SLG of different underlying substrates. Reaction time = 10 min, [NBD] = [KI] = 10 mM. (a) Raman spectra of pristine and functionalized SLG/Cu. (b) Raman spectra of pristine and functionalized SLG/Au.

XPS Analysis

Spectra were recorded on a Kratos Axis Supra X-ray Photoelectron Spectrometer employing a monochromatized Al K α ($h\nu = 1486.7$ eV, 150 W) X-ray source, hybrid (magnetic/electrostatic) optics with a slot aperture, hemispherical analyser, multichannel plate and delay line detector (DLD) with an emission angle of 0° relative to the sample surface normal. Survey spectra were acquired with a pass energy of 160 eV and high-resolution spectra with 20 eV. The resulting spectra were processed using CasaXPS software. Binding energy was referenced to Ag 3d_{5/2} at 368.21 eV measured on sputter cleaned silver under the same analysis conditions, on the same day as the samples. Good electrical contact between the graphene layer and the spectrometer was ensured by use of silver paint “track” from the top of the sample to the sample bar. Components in high resolution spectra were fitted using the “LA(α, m)” lineshape for symmetric peaks and the “LF(α, β, w, m)” line-shape for asymmetric peaks corresponding

to a numerical convolution of Lorentzian functions (with exponents α and β for the high binding energy and low binding energy sides) with a Gaussian (width m) and inclusion of tail-damping (w) to provide finite integration limits. Details of these lineshape functions are available in the CasaXPS documentation online.⁷

Empirical relative sensitivity factors supplied by Kratos Analytical (Manchester, UK) were used for quantification. Use of these relative sensitivity factors does not account for any attenuation due to overlayers or other surface contamination and assumes a uniform depth distribution of elements within the information depth of the sample. Matrix effects are also discounted.^{8,9} Quoted standard deviations result from Monte Carlo simulations of the error in peak modelling and discount all other (potentially larger) sources of error.

During fitting of the carbon 1s spectra the following constraints were made in order to provide a stable and meaningful fit to the experimental data:

1. The lineshape used for the C=C graphene peak was left unchanged between the unmodified graphene and NBD functionalized graphene samples.
2. The FWHM was fixed for all symmetric component peaks ascribed to species associated with the nitrophenyl moiety, oxidation or C-C defects in the graphene substrate.
3. The relative intensity of the C-NO₂ and C=C (nitrophenyl) peaks were fixed to correspond with the ratio expected from the nitrophenyl moiety.
4. The C-C (defect) component binding energy was fixed at 285.0 eV.

Survey spectra of the samples (Fig. S2) revealed the expected carbon, nitrogen (for the NBD grafted sample), oxygen and silicon. Additionally, a low concentration of iron was present in both the unmodified and NBD grafted graphene samples. The origin of this iron species is unknown. The NBD grafted graphene also showed a low level of iodine contamination from the grafting process.

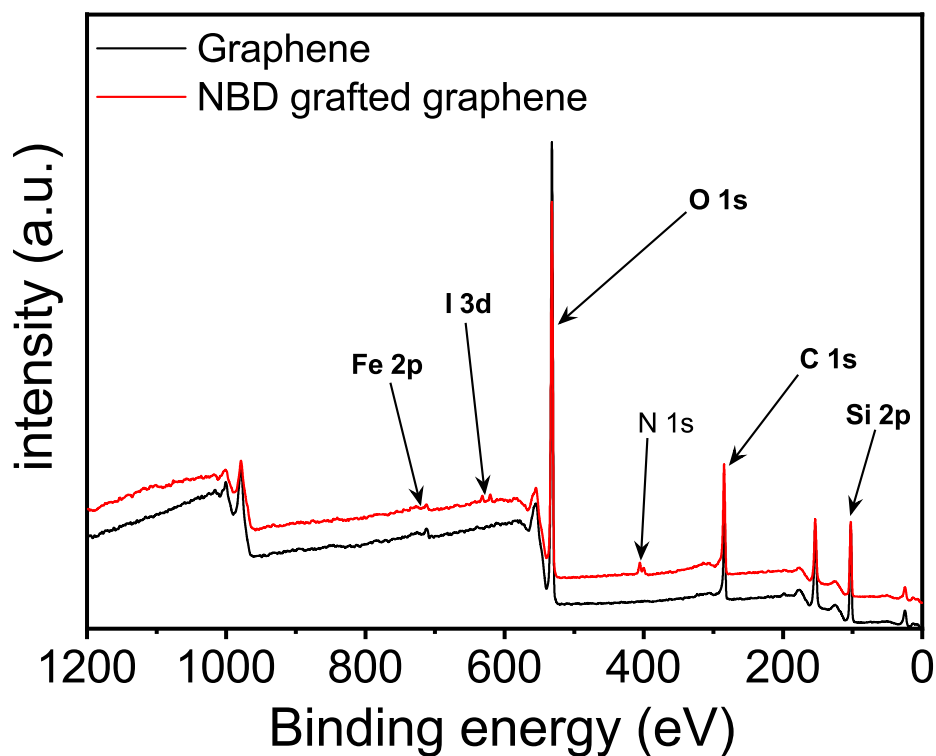


Fig. S3. XPS Survey spectra of unmodified SLG/SiO₂ (black) and NBD functionalized SLG/SiO₂ (red).

Table S2: Data derived from carbon 1s high resolution spectra of the graphene samples

Component	Binding energy /eV	FWHM /eV	Area /%	St. Dev. /%
Pristine SLG/SiO₂				
C=C graphene	284.1	0.84	90.56	0.73
C-O	286.2	0.92	0.68	0.10
$\pi^* \leftarrow \pi$	290.2	4.66	6.43	0.44
$\pi^* \leftarrow \pi$	294.3	3.77	2.34	0.91
NBD functionalized SLG/SiO₂				
C=C graphene	284.2	0.80	44.92	0.46
C=C nitrophenyl	284.8	1.30	24.66	0.25
C-C	285.0	1.30	4.06	0.18
C-NO ₂	285.6	1.30	4.93	0.05
C-O	286.2	1.30	8.41	0.25
C=O/C-NH ₃ ⁺	287.6	1.30	1.94	0.18
O-C=O	288.7	1.30	1.15	0.22
$\pi^* \leftarrow \pi$	290.5	2.89	3.94	0.23
$\pi^* \leftarrow \pi$	292.9	4.87	6.00	0.65

The nitrogen 1s high resolution spectrum (Fig. S3) of the NBD functionalized graphene sample shows significant reduction of the nitro group to amines, protonated amines and other nitrogen containing species. This has previously been linked to photochemical reduction of nitrobenzene by X-ray irradiation,¹⁰ however, tests of X-ray induced reduction on multiple sample areas show that this was not a significant contributor to the reduced nitrogen environments in this dataset. The nitrogen 1s data is summarized in Table S3.

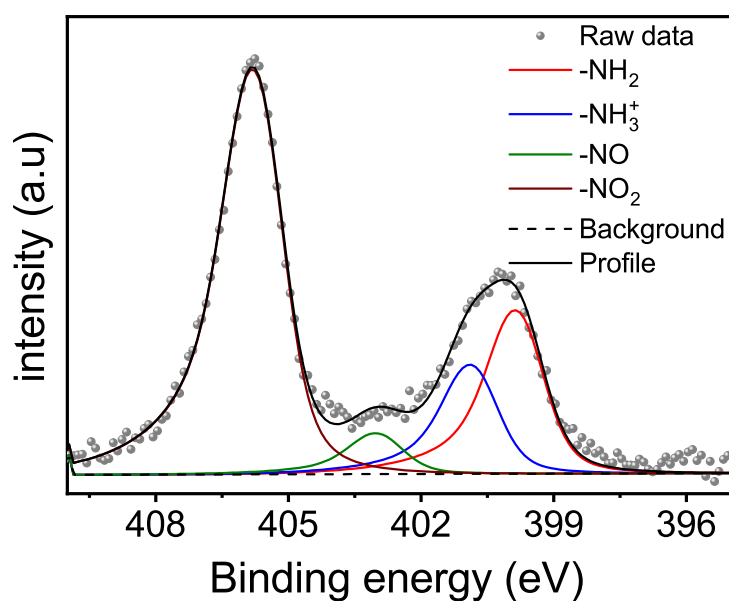


Fig. S4. Nitrogen 1s high resolution spectrum of NBD functionalized SLG/SiO₂.

Table S3. Data for nitrogen 1s spectrum of NBD functionalized SLG/SiO₂.

Component	Binding energy /eV	FWHM /eV	Area /%	St. Dev. /%
-NH ₂	399.8	1.43	20.63	1.68
-NH ₃ ⁺	400.8	1.43	13.21	2.08
-NO	403.0	1.43	4.70	0.89
-NO ₂	405.7	1.43	61.46	2.16

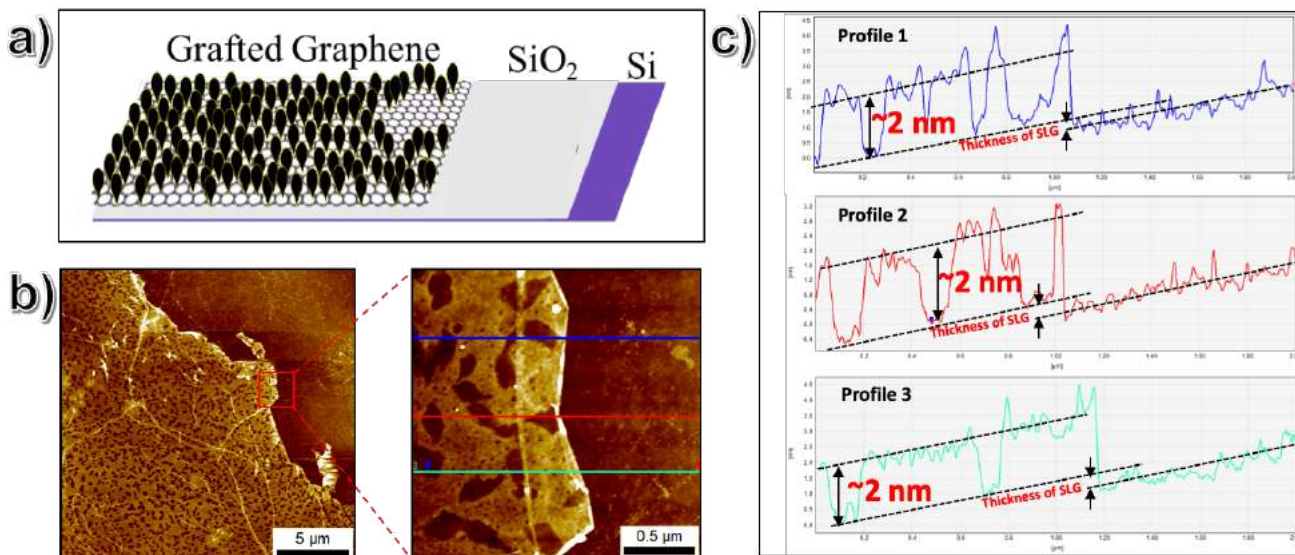


Fig. S5. AFM images showing the edge of functionalized SLG-SiO₂ and the corresponding topographical line-profiles reflecting the layer thickness of functionalization layer. (a) Schematic illustration of the edge of functionalized SLG-SiO₂. (b) The edge of functionalized SLG-SiO₂ characterized by AFM. Three line-profiles performed based on the amplified edge of functionalized SLG-SiO₂. (c) The corresponding line-profiles reflecting the layer thickness of functionalization layer. The height of the functionalization layer, graphene and silica substrate indicate that the bottom of the empty areas (corrals) within the functionalization layer is graphene.

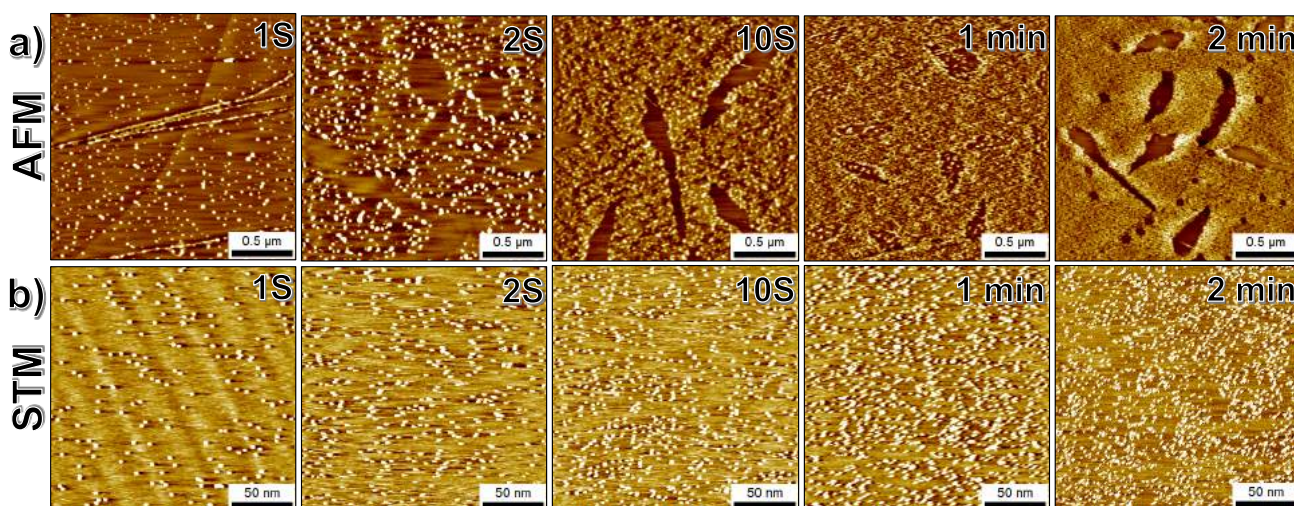


Fig. S6. Additional AFM (a) and STM (b) data for the dependence of reaction time on covalent grafting of NBD. [KI] = 10 mM, [NBD] = 10 mM. STM data shows typical bright features that arise from grafted molecules even when the droplet of the reaction mixture is washed away within a second or two seconds from the surface highlighting the efficiency of the functionalization process. Tunneling parameters in STM: (2 s) $I_{set} = 0.1$ nA, $V_{bias} = -0.6$ V; (10 s) $I_{set} = 0.07$ nA, $V_{bias} = -0.5$ V; (1 min) $I_{set} = 0.1$ nA, $V_{bias} = -0.5$ V; (6 min) $I_{set} = 0.05$ nA, $V_{bias} = -0.82$ V.

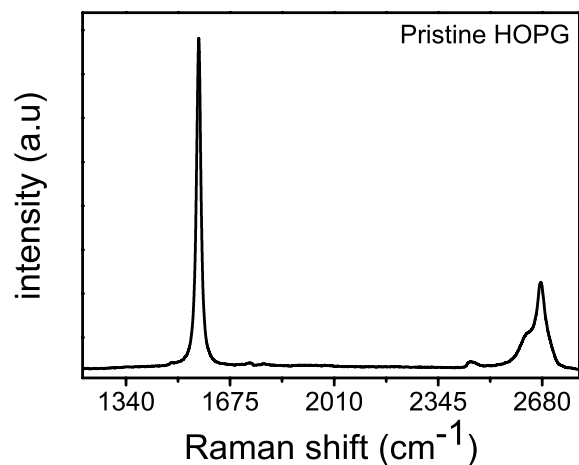


Fig. S7. Raman spectrum of the pristine HOPG surface prior to functionalization. The absence of the D band indicates that the intrinsic defect density on unfunctionalized HOPG samples is low.

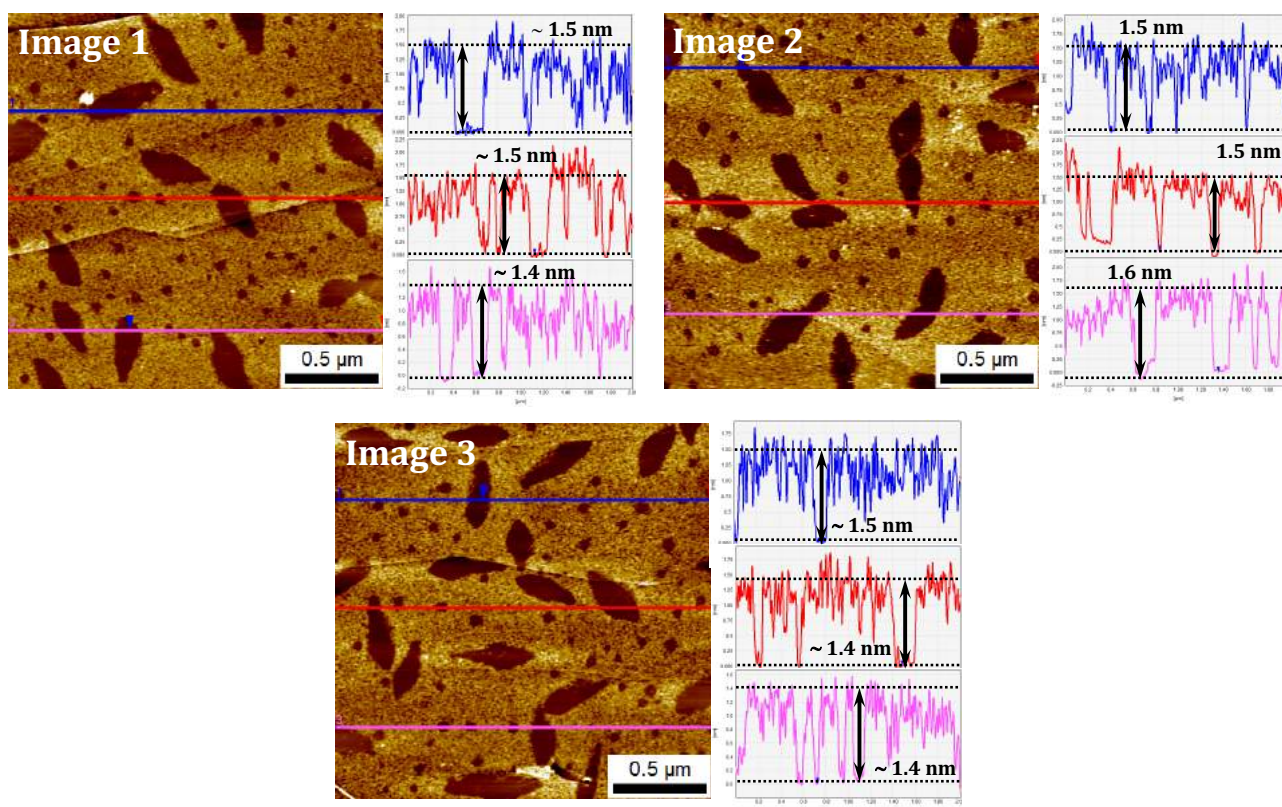


Figure S8. Representative AFM data set showing how average topographical height of the covalently grafted films was obtained. Typically, between 3 to 5 AFM images obtained on different parts of same sample were considered for height analysis. Within these images, height profiles were measured across three different locations and the measured values were averaged. The average thickness of the film for this data set is 1.5 ± 0.1 nm. Reactions conditions for this data set: 10 mM KI, 10 mM NBD, reaction time = 10 min. The AFM data obtained on all other samples was treated using the same approach.

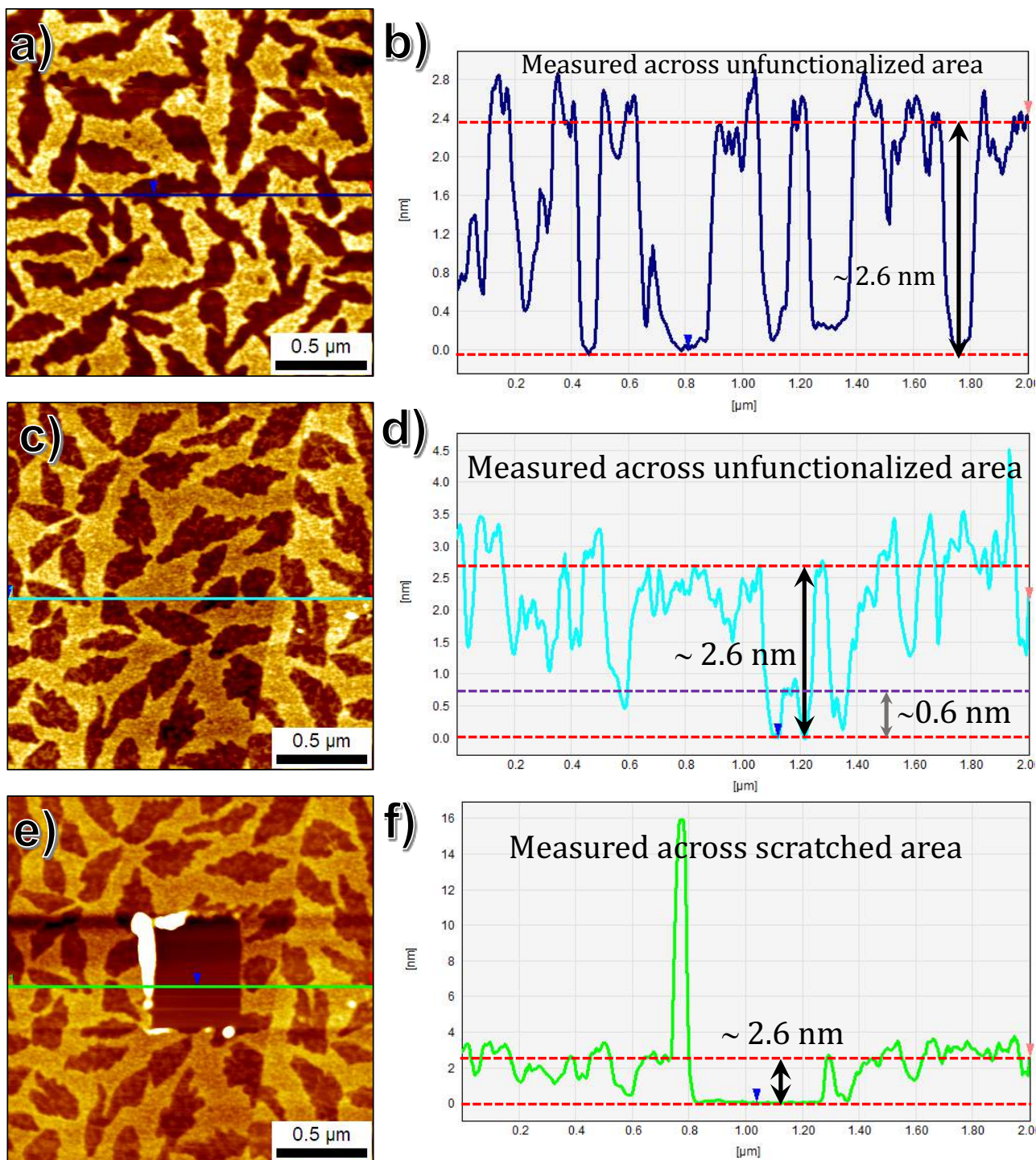


Fig. S9. Comparison between the layer thickness obtained using topographical height measured across (a, b) unfunctionalized areas with no physisorbed deposits, (c, d) unfunctionalized areas with physisorbed deposits and (e, f) an area obtained *via* scratching away the film using the AFM tip in contact mode (same area as that in c). Reaction conditions: 50 mM KI, 50 mM NBD, reaction time = 10 min. The unmodified areas seen in panel (c) are possibly occupied by some physisorbed material. The topographical height of the physisorbed deposit is around 0.6 nm as evident from height profile provided in panel (d).

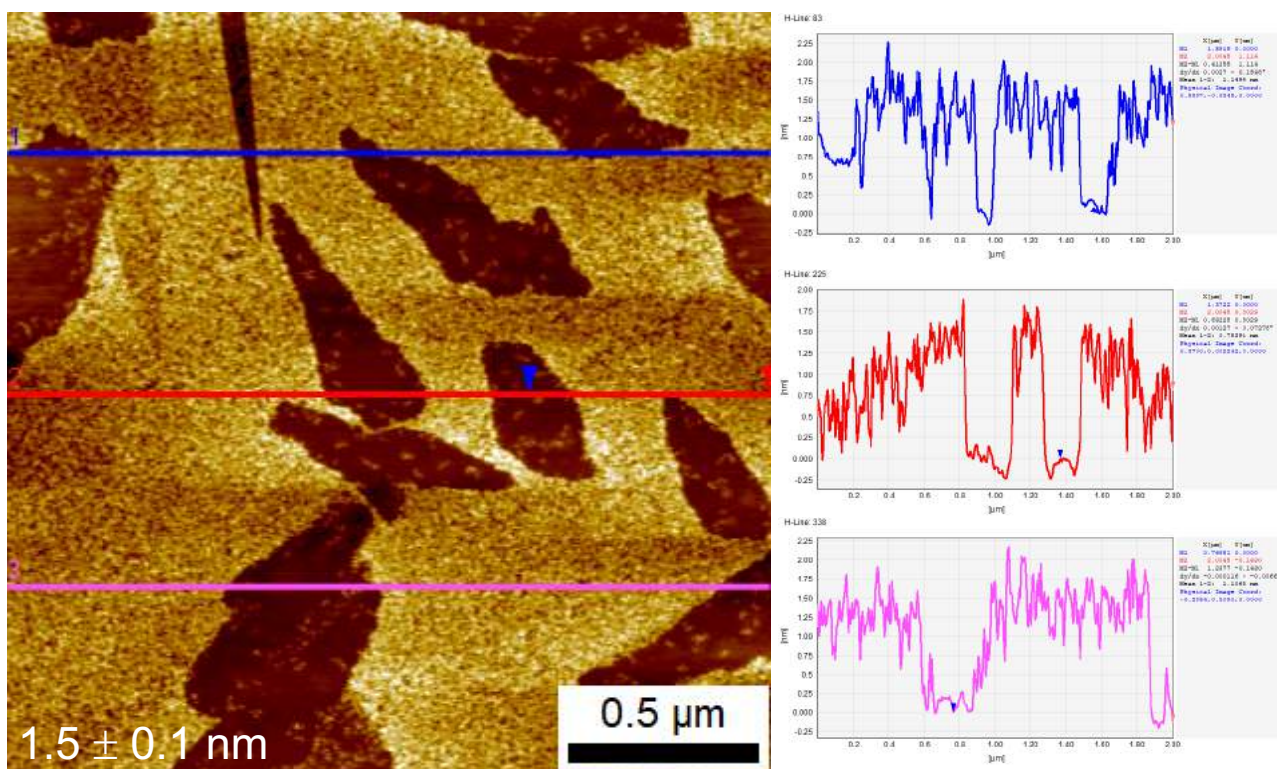


Fig. S10. A representative AFM image showing that an increase in the reaction time to 30 minutes does not lead to any further increase in the layer thickness than that obtained at 10 minutes. The layer thickness for this sample was found to be around 1.5 ± 0.1 nm which is comparable to that obtained using shorter reaction (10 min) times using the same concentration of reagents.

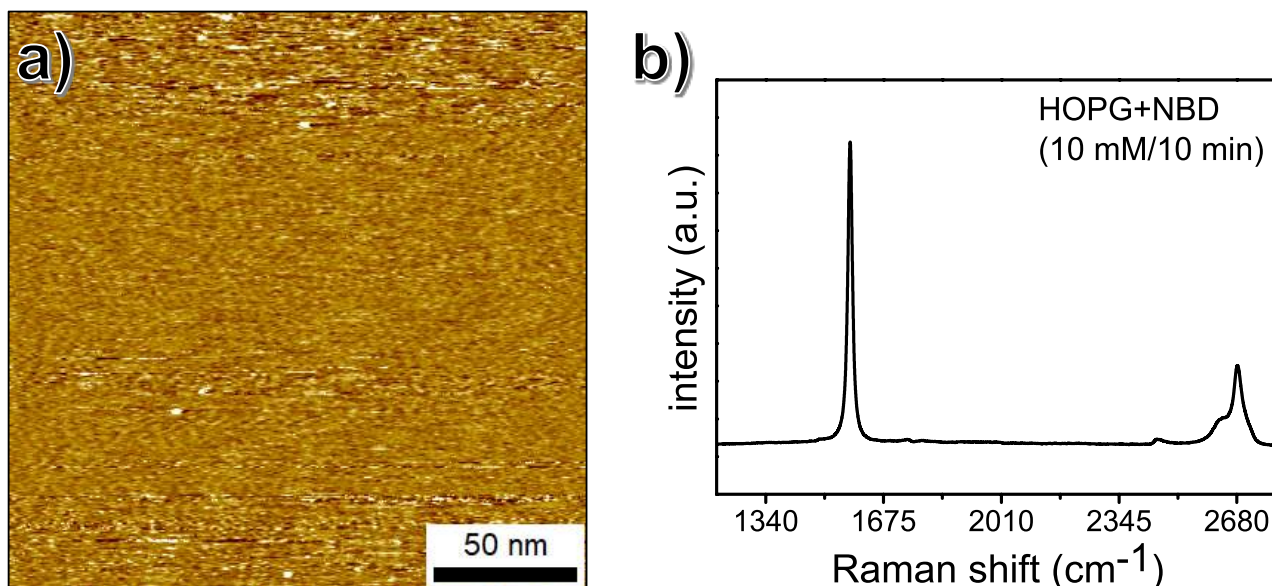


Fig. S11. Spontaneous reaction of NBD with the HOPG surface. (a) A representative STM image showing absence of grafted film on the HOPG surface. (b). Raman spectrum of the HOPG surface allowed to spontaneously react with NBD (10 mM) for 10 min.

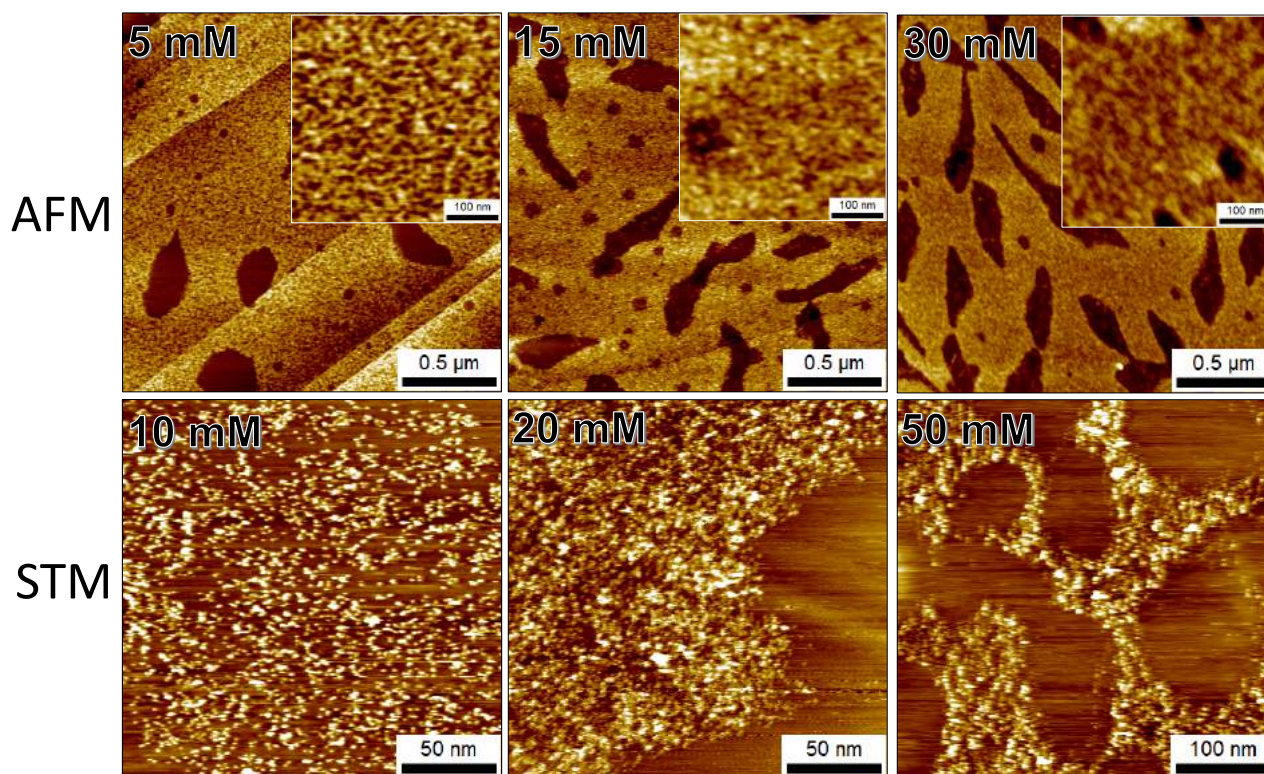


Fig. S12. Additional AFM and STM data for the dependence of NBD concentration on the covalent grafting of NBD. $[\text{NBD}]/[\text{KI}] = 1:1$ and reaction time = 10 min. The STM images are provided for those concentrations for which AFM data is provided in the main text.

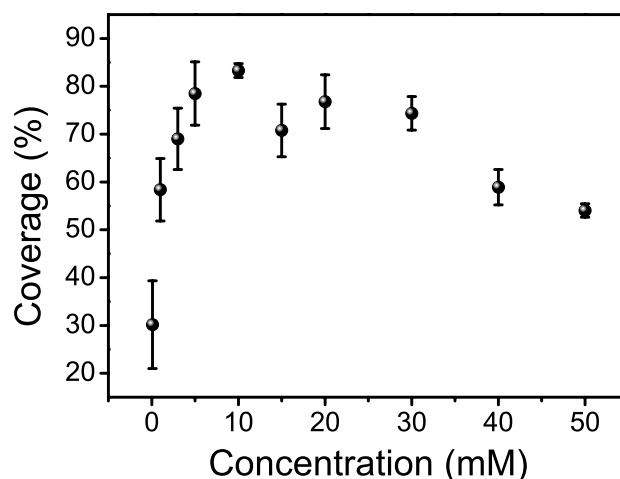


Fig. S13. Variation in the surface coverage of the covalently grafted film as a function of NBD concentration as measured from AFM images. KI was used in equimolar amount. The reaction time was kept constant at 10 min. The surface coverage of the grafted films was obtained by measuring the area of the empty unfunctionalized regions. Each value for surface coverage was obtained by estimating the surface coverage of the empty areas from 5 AFM images ($2 \mu\text{m} \times 2 \mu\text{m}$) and then calculating the surface coverage of the film.

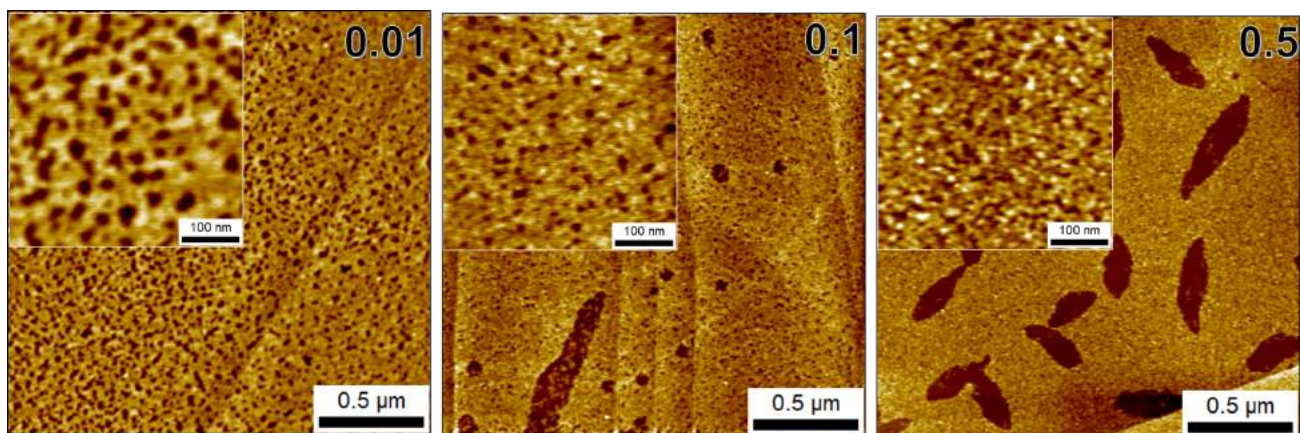


Fig. S14. Additional AFM data for the [KI]/[NBD] solution mole ratio on covalent grafting on the surface of HOPG. [NBD] = 10 mM and reaction time = 10 min.

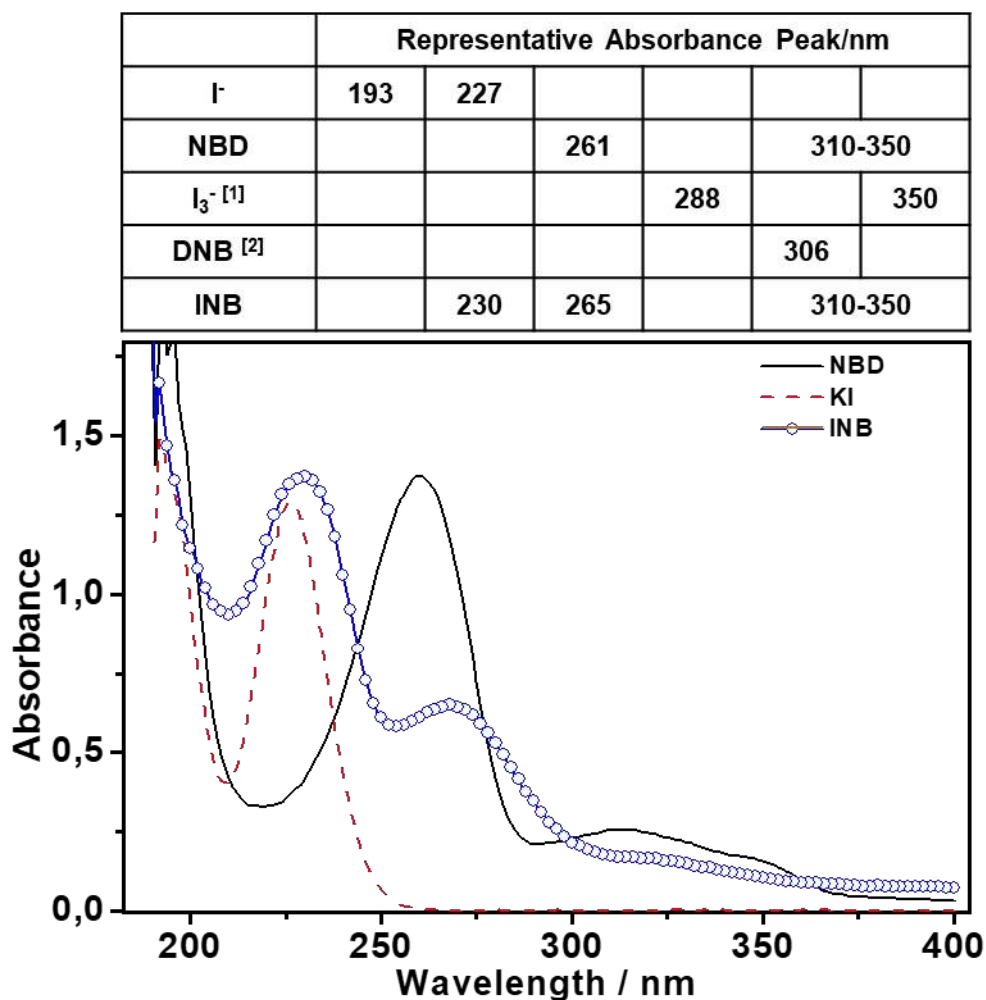


Fig. S15. UV-Vis spectra for NBD, KI and a potential by-product of the reaction 1-iodo-4-nitrobenzene (INB). The absorption maxima for triiodate (I₃⁻)¹¹ and 4,4'-dinitro-1,1'-biphenyl (DNBP)¹² have been reported earlier.

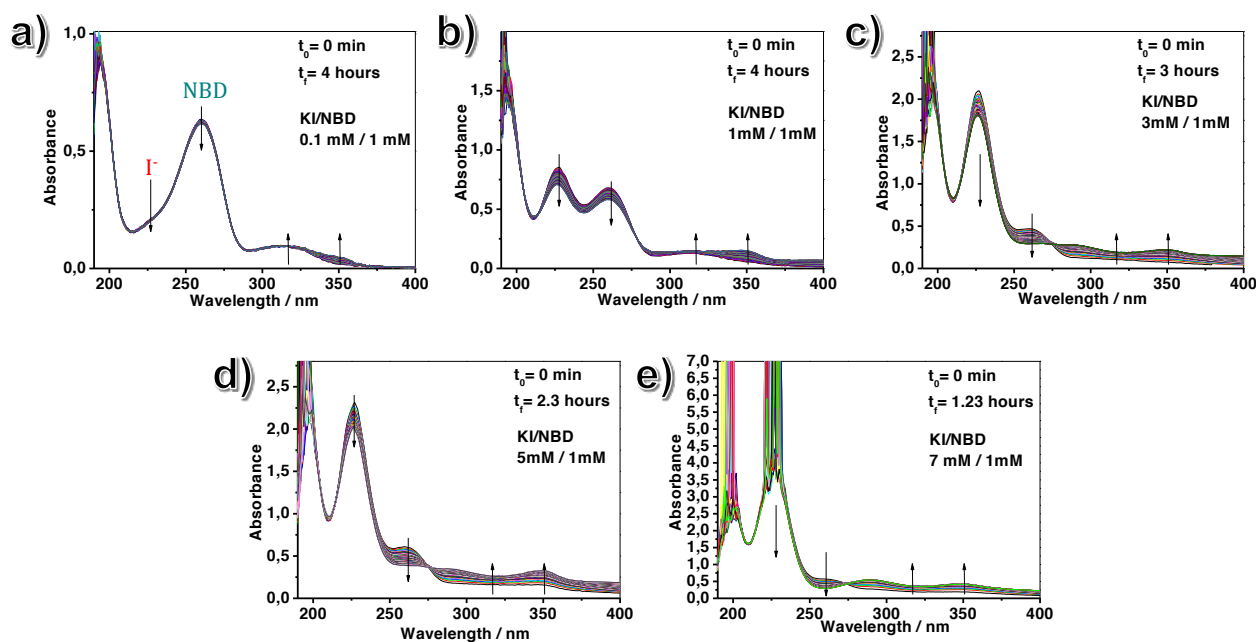


Fig. S16. The time evolution of the UV-vis absorbance of the reaction mixture at different $[KI]/[NBD]$ ratios in aqueous solution. In all cases the NBD concentration is fixed at 1 mM and KI concentration was varied from 0.1 mM (a) to 7 mM (e).

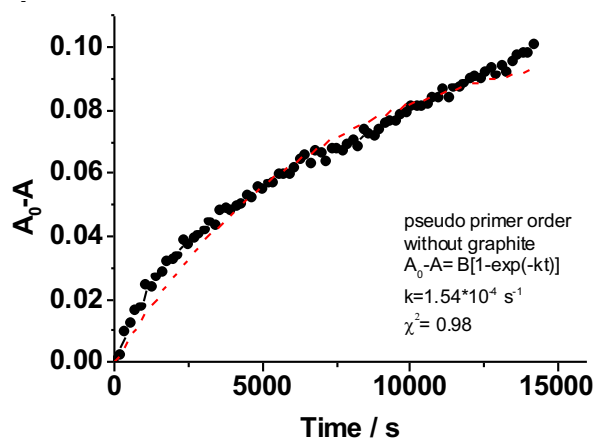


Figure S17. Time evolution of the UV-vis absorbance of NBD and KI. The dashed line represents the best fit for 1st order kinetics $[A-A_0 = B[1-\exp(-kt)]]$. In this equation k is the reaction rate constant for the system and B is defined as function of the optical path length (l) and the difference between the molar extinction coefficient ($B = lc_0(\epsilon_1 - \epsilon_f)$).

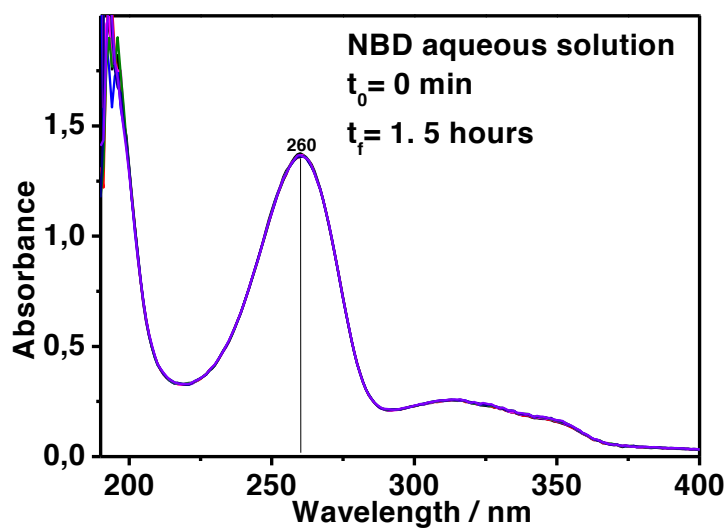


Fig. S18. Absorption spectrum of aqueous NBD as a function of time (monitored over a period of 1.5 hours). The absorbance of aqueous NBD solution does not change much indicating extremely slow rate of decomposition in the absence of either KI or graphite powder.

References:

- 1 T. Wei, M. Kohring, M. Chen, S. Yang, H. Weber, F. Hauke, and A. Hirsch, *Angew. Chem. Int. Ed.*, **2020**, *59*, 1–6.
- 2 Q. Wang, Z. Jin, K. Kim, A. Hilmer, G. Paulus, C. Shih, M. Ham, J. Sanchez-Yamagishi, K. Watanabe, T. Taniguchi, J. Kong, P. Jarillo-Herrero and M. Strano, *Nat. Chem.*, **2012**, *4*, 723–732.
- 3 J. Englert, C. Dotzer, G. Yang, M. Schmid, C. Papp, J. Gottfried, H. Steinruck, E. Spiecker, F. Hauke and A. Hirsch, *Nat. Chem.*, **2011**, *3*, 279–286.
- 4 T. Wei, O. Martin, S. Yang, F. Hauke, and A. Hirsch, *Angew. Chem. Int. Ed.* **2019**, *58*, 816–820.
- 5 Z. Sun, C. Pint, D. Marcano, C. Zhang, J. Yao, G. Ruan, Z. Yan, Y. Zhu, R. Hauge and J. Tour, *Nat. Commun.* **2011**, *2*, 559.
- 6 G. Abellañ, M. Schirowski, K. Edelthammer, M. Fickert, K. Werbach, H. Peterlik, F. Hauke, and A. Hirsch, *J. Am. Chem. Soc.* **2017**, *139*, 5175–5182.
- 7 N. Fairley, Lorentzian Asymmetric Lineshape, http://www.casaxps.com/help_manual/manual_updates/LA_Lineshape.pdf, (accessed 2 September 2017).
- 8 D. Briggs and J. T. Grant, Eds., *Surface Analysis by Auger and X-ray Photoelectron Spectroscopy*, IM Publications, Manchester, 2003.

- 9 S. Hofmann, Auger- and X-Ray Photoelectron Spectroscopy in Materials Science, Springer Berlin Heidelberg, Berlin, Heidelberg, 2013, vol. 49.
- 10 K. Roodenko, M. Gensch, J. Rappich, K. Hinrichs, N. Esser and R. Hunger, *J. Phys. Chem. B*, **2007**, *111*, 7541–7549.
11. A. E. Burgess and J. C. Davidson. *J. Chem. Edu.* **2012**, *89*, 814-816.
12. Bio-Rad Laboratories, Inc. SpectraBase; SpectraBase Compound ID=639lhqsWLzp SpectraBase Spectrum ID=KxKsK2Msvsa <http://spectrabase.com/spectrum/KxKsK2Msvsa> and Dorr, F.; Gazis, E., UV atlas of organic compounds, 1966, 1, D10/6.